Hindawi
International Journal of Antennas and Propagation
Volume 2022, Article ID 4728303, 21 pages
https://doi.org/10.1155/2022/4728303

Review Article

Progress and Challenges in Electromechanical Coupling of Radio Telescopes

Yuefei Yan,[1] **Song Xue**,[1] **Xinlan Hu**,[1] **Peiyuan Lian**,[1] **Qian Xu**,[2] **Na Wang**,[2] **Wulin Zhao**,[3] **Yang Wu**,[4] **Baoyan Duan**,[1] **and Congsi Wang**[1]

[1]*Key Laboratory of Electronic Equipment Structure Design, Ministry of Education, Xidian University, Xi'an 710071, China*
[2]*Xinjiang Astronomical Observatory, China Academy of Sciences, Urumqi 830011, China*
[3]*The 39th Research Institute of China Electronics Technology Group Corporation, Xi'an 710065, China*
[4]*The 54th Research Institute of China Electronics Technology Group Corporation, Shijiazhuang 050081, China*

Correspondence should be addressed to Song Xue; sxue@xidian.edu.cn and Congsi Wang; congsiwang@163.com

Received 3 April 2022; Revised 31 October 2022; Accepted 11 November 2022; Published 22 November 2022

Academic Editor: Mohammad Alibakhshikenari

Radio astronomy is a discipline of dynamics and wonders. The vast universe has many secrets to unravel. As one of the important facilities in this discipline, radio telescopes play a key role in collecting astronomical data and unraveling mysteries. With the demand of radio astronomy for a higher frequency, wider bandwidth, higher gain, and higher pointing accuracy, the aperture of the radio telescope is gradually increasing, and its electrical performance and structure have become tightly coupled. Therefore, how to ensure the stable and efficient operation of the telescope for the long-term operation has become the urgent demand for large aperture high-performance radio telescopes. Therefore, this paper firstly makes a comparison of the overall condition of large radio telescopes in nearly a decade that are both constructed and operated, including the progress of radio telescopes that are being constructed and the planning for construction. Then, systematically summarized the latest research progress of electromechanical coupling technology from 3 aspects of connotation and application of electromechanical coupling, and performance guarantee under slowly varying load and performance guarantee under rapidly varying load from the perspectives of design, manufacturing, and observation operating. Lastly, the future research direction of electromechanical coupling technology is pointed out according to the development trend of radio astronomy.

1. Introduction

Many major astronomical discovery projects in recent years involve the radio telescope. For example, in the original gravitational wave discovery in 2014 [1, 2], scientists used a 10 m aperture South Pole Telescope (SPT, located in Antarctica). In 2017, the European Southern Observatory used 4 Very Large Telescopes (VLTs) in Chile to observe the merger of two neutron stars [3]. Behind the first black hole photo taken in 2019, a total of 8 telescopes (or telescope arrays) are combined into the Event Horizon Telescope (EHT) for global observation [4]; these telescopes include the Atacama Large Millimeter/submillimeter Array (ALMA, located in Chile with 54 12 m and 12 7 m aperture radio telescopes), the Atacama Pathfinder Experiment Telescope (APEX, 12 m aperture, located in Chile), the James Clerk Maxwell Telescope (JCMT, 15 m aperture, located in Hawaii), the Submillimeter Array, SMA, located in Hawaii with 8 6 m aperture radio telescopes), the Submillimeter Telescope (SMT, 10 m aperture, located in Arizona, USA), the Large Millimeter Telescope (LMT, 50 m aperture, located in Mexico), the Pico Veleta Telescope (PVT, 30 m aperture, located in Spain), and the SPT as mentioned earlier in the article. In 2020, the European VLBI Network (EVN) used eight other telescopes to observe multiple repeated fast radio burst sources [5], including the Effelsberg Telescope (100 m aperture, located in Germany), the Tianma Telescope (65 m aperture, located in Shanghai, China), the Medicina Telescope (32 m aperture, located in Italy), the Toruń Telescope (32 m aperture, located in Poland), the Irbene Telescope

(32 m aperture, located in Latvia), the Jodrell Bank Mark II (25 m ∗ 38 m, located in the UK), the Onsala Telescope (25 m aperture, located in Sweden), and a telescope in the Westerbork array (a total of 11 25 m aperture radio telescopes, located in the Netherlands).

In these discoveries, radio telescopes have played a crucial role. When making astronomical observations, celestial objects can not only be observed in visible light but also radiate radio waves [6]. As the device for receiving these radio waves, a large antenna body is the most obvious feature of the radio telescope [7]. As a typical electromechanical coupling device, the antenna body of a radio telescope consists of two parts, electrical and mechanical. An antenna is installed on the base of each radio telescope, and at least one receiving device is used to detect signals. The structural part of the antenna is not only the carrier and guarantee for the realization of the electrical performance of the antenna but also often restricts the realization of the electrical performance [8]. Reflector antennas are an ideal type of radio telescopes, which reflect radio waves well to a single point. With the continuous development of radio astronomy, the high sensitivity and high-resolution requirements of the antenna system need to increase the effective receiving area of the antenna while ensuring surface accuracy [9], which means that the aperture of the reflector antenna needs to be increased. With the increase of the antenna aperture, the weight of the antenna structure increases dramatically. The large weight makes it increasingly difficult to ensure the stiffness of the antenna structure [10]. Meanwhile, the improvement of the working frequency of the antenna also requires an unprecedented degree of reflector surface accuracy [11]. Its design operating frequency is up to 115 GHz, and the surface root mean square error (RMSE) is required to reach 0.2 mm. Such high accuracy requirements have brought unprecedented challenges to the design of large aperture antenna structures.

The mutual influence and restriction of the electrical performance and mechanical structure of the radio telescope have made the development cycle of the large-aperture high-performance single-dish antenna relatively long. At the same time, the complex observation environment makes the operation and maintenance of the telescope quite difficult. Thus, this paper first outlines the development of radio telescopes in recent years, including major constructions that are completed and under construction or in preparation for construction, then summarizes the key technologies of electromechanical coupling of radio telescopes from two aspects of design manufacturing and observation operating and analyze the key technologies one by one. On this basis, the research hotspots of radio telescopes in future developments are discussed at last to provide a technical reference for the efficient operation and maintenance of radio telescopes.

2. Development Trends of Radio Telescopes in Recent Years

The large radio telescopes in service in the world, in addition to those mentioned in the introduction, also include the Green Bank Telescope (GBT, 100 m × 110 m aperture, located in West Virginia, USA), the Sardinia Radio Telescope (SRT, 64 m aperture, located in Italy), Nobeyama Telescope (45 m aperture, located in Japan), the Lovell Telescope (76 m aperture, located in UK), Parkes Radio Telescope (64 m aperture, located in Australia), Yebes Telescope (40 m diameter, located in Spain), as well as the 26 m Nanshan Telescope located in Urumqi, Xinjiang, China, the 40 m Telescope located in Kunming, Yunnan, and the 50 m Telescope located in Miyun, Beijing, etc. These telescopes have been summarized in detail in [6, 7, 9]; thus the authors give no further elaborations. In addition, the Arecibo Telescope (305 m aperture, located in the U.S. island of Puerto Rico), the second largest single-dish fixed radio telescope in the world, crashed due to the suspended electrical receiving part after nearly 60 years of service, and the main body of the reflector surface was also damaged, this telescope has officially retired at the end of 2020.

This section will focus on the development of various radio telescopes that have been constructed and put into operation in recent years, as well as those under construction and be constructed in the future. The authors have drawn a map to better exhibit the distribution of the major radio telescopes in the world according to their geographical distribution and types (Figure 1).

2.1. Radio Telescopes Being Constructed and Put into Operation in Recent Years

2.1.1. Radio Telescope at Kashgar Deep Space Station, China. The Kashgar Deep Space Measurement and Control Station in Xinjiang, China, is one of the three deep space measurement and control stations in the Chinese deep space measurement and control network. The other two are located in Jiamusi, Heilongjiang, and Argentina [12]. The Kashgar Deep Space Station was built and put into use in 2013. At first, there was only a set of 35 m reflector antennas capable of measuring and controlling the three frequency bands of *S*/*X*/*Ka* (Figure 2(a)). By the end of 2020, the Kashgar Deep Space Station has built three new antennas with an aperture of 35 m (Figure 2(b)), which consists Chinese first deep space antenna array system along with the original 35 m antenna. Its data-receiving capability is equivalent to that of the 66 m aperture antenna. After the official launch of the deep space antenna array system, it was directly put into the measurement and control missions of Tianwen-1 and Chang'e-4. It is worth mentioning that Queqiao, as the relay communication satellite of the Chang'e-4 lunar probe, carries a 4.2 m aperture deployed antenna, which is the largest antenna used in deep space exploration missions domestica and abroad [13]. Meanwhile, Queqiao is the Chinese first and the world's first relay satellite operating in extraterrestrial orbit.

2.1.2. Radio Telescope of Jiamusi Deep Space Station, China. Jiamusi Deep Space Station (Figure 3), located in Heilongjiang Province, China, was constructed and put into

Figure 1: Distribution of radio telescopes.

operation in 2013. It has a reflector antenna with an aperture of 66 m and was the largest deep space exploration antenna in China at that time [14]; it works in the *S*/*X* frequency band. The antenna adopts the Cassegrain form and beam waveguide feeding. The main reflecting surface is a combination of solid panel and mesh panel design, which greatly reduces the structural deformation caused by the weight of the antenna. Since the Jiamusi Deep Space Station was put into use, together with the Kashgar Deep Space Station, it has escorted China's aerospace industry for a long time and provided measurement and control support for the Chang'e 3, 4, and 5 satellites as well as the Tianwen-1 probe.

2.1.3. Radio Telescope of Argentina Deep Space Station, China. During the launch of the Tianwen-1 Mars probe, the Argentine Deep Space Station took the lead in capturing the probe's target. The probe was subsequently successfully captured by Jiamusi Deep Space Station and Kashi Deep Space Station. In 2014, China signed a contract with the Argentine government to build the first overseas deep space measurement and control station in Las Lajas, Neuquén province in western Argentina (Figure 4). In 2017, the Argentine Deep Space Station was built and put into operation using a set of deep space measurement and control equipment with the abilities of working in three frequency bands of *S*/*X*/*Ka* [12]. After the construction of the Argentine deep space station, China has built a deep space exploration network with *S*/*X*/*Ka* multifrequency band measurement and control capabilities, integrating measurement and control, data transmission, interferometry, continuous TT and C, reliable communication, and precise navigation services with very high performance [15]. The coverage rate of deep space spacecraft has increased to more than 90%, and the comprehensive level is at the forefront of the world [16].

2.1.4. Tianma 65 m Radio Telescope in Shanghai, China. The Tianma 65 m telescope (Figure 5), located in Sheshan, Songjiang, Shanghai, was set up in the project in 2008 [17], and its design and construction began in 2009. The first stage of construction was completed in 2012, and it has VLBI observation capabilities in *S*/*X*, *L*, and *C* bands [18]. By 2016, receivers in the *Ku*, *X*/*Ka*, and *K* bands were added. The main reflector of the antenna adopts the best matching-shaped double reflector. The subreflector adopts the six-bar parallel mechanism adjustment technology to achieve high-precision adjustment of five degrees of freedom [19]. In addition, Tianma Telescope is the first radio telescope in China equipped with an active surface system. After the active surface system is turned on, the surface shape accuracy can be better than 0.3 mm. The Tianma Telescope has completed the Chang'e series of missions and Mars exploration missions with high quality during the operation phase and completed the overall acceptance in 2017. It is currently actively serving domestic radio astronomy observations.

2.1.5. Haoping 40 m Radio Telescope in Shaanxi, China. The Haoping Observatory of the National Service Center of the Chinese Academy of Sciences is in Luonan, Shaanxi Province. It has a 40 m aperture reflector antenna (Figure 6), which is mainly used to track and receive downlink signals from GNSS (Global Navigation Satellite System) satellites to achieve high GNSS satellite signal accuracy in observation

and analysis [20], and will also be used to carry out radio astronomy observations such as pulsars and spectral lines etc. [21], and VLBI work is also planned in the future [22]. At present, based on the radio telescope, research on the time scale of pulsars is being carried out, and long-term timing observations have been carried out on many high-precision millisecond pulsars.

2.1.6. Wuqing 70 m Radio Telescope in Tianjing, China. After the Zhurong Mars probe landed on Mars, the signal sent back by the probe was extremely weak due to the long distance of 400 million kilometers between Earth and Mars. To ensure the steady operation of the Mars probe, the National Astronomical Observatory of the Chinese Academy of Sciences built a 70 m aperture antenna in Wuqing, Tianjin province, as a high-performance receiving system, mainly working in the *S*/*X*/*Ku* band. Its highly symmetrical umbrella support structure design makes the reflector deformation more uniform, to achieve the effect of equal flexibility support [23]. The overall installation of the reflector was completed in April 2020. The acceptance was completed in February 2021, and together with the Beijing Miyun 50 m antenna and the Yunnan Kunming 40 m antenna, it was in charge of receiving the return data of Tianwen-1 [24]. The completion of the Wuqing 70 m antenna (Figure 7) makes it the largest single-dish steerable antenna in Asia.

2.1.7. Five Hundred-Meter Aperture Spherical Radio Telescope (FAST). After the retirement of the Arecibo telescope, FAST became the only "eye for the sky" in the world. The 500-meter aperture spherical radio telescope in Pingtang, Guizhou Province, is currently the largest radio telescope in the world with the highest degree of sensitivity (Figure 8). Its site selection and preresearch began in 1994 [25]. The project was approved in November 2002, then started construction in 2011, and was completed in September 2016. After nearly 4 years of commissioning and trial operation, it passed the national acceptance in January 2020. This enormous project took 26 years to complete. It adopts a Gregorian feed cabin to collect signals. Compared with the Arecibo telescope, there are three main innovations. Firstly, the karst landform of the selected site is very consistent with the construction conditions of the giant single-aperture telescope. Secondly, it is active optics technology. Each panel of the reflector is equipped with a real-time active controller. The active control system can form a 300 m aperture instantaneous parabolic surface in the direction of celestial observation. Finally, the light cable-driven feed cabin technology of optical-mechanical-electrical integration makes the flexible connection between the feed and the reflector to achieve high-precision pointing and tracking. Over 100 new pulsars were discovered using FAST during the commissioning and trial operation phase [26]. FAST mainly operates between 70 MHz and 3 GHz, and compared with Arecibo, the scanning speed is three times faster in the L-band and the sky coverage range is two times wider [27]. The successful construction and operation of FAST are playing a significant role in the field of radio astronomy.

2.1.8. Greenland Telescope. The Greenland Telescope (GLT) is located in the northwest of Greenland. It is a 12 m aperture antenna working in the millimeter/submillimeter band (Figure 9). The antenna is the prototype of ALMA, originally located in Chile, and later gifted by the US National Science Foundation to the Academia Sinica Institute of Astronomy and Astrophysics (ASIAA) [28]. After upgrading, the construction was completed and put into operation in 2017. The main reflector is equipped with a deicing device. The servo system is based on the ALMA antenna system using two high-precision tiltmeters, one on the azimuth bearing and the other on the support cone. The antenna is currently mainly involved in the VLBI observation of the M87 galaxy [29, 30].

2.1.9. Thai National 40 m Radio Telescope. The 40 m Thai National Radio Telescope (TNRT) was proposed by the National Astronomical Institute of Thailand in 2017 and was assembled in 2020 (Figure 10). TRNT has been put into use in early 2022. Its most important difference is its main focus on low-frequency or phased array feed systems. It is mainly used for astronomical observations such as pulsars, fast radio bursts, star-forming regions, galaxy, and active galactic nuclei, et al. As a single-dish instrument, TNRT is a perfect tool to explore time domain astronomy with its agile observing systems and flexible operation. Due to its ideal geographical location, TNRT will significantly enhance Very Long Baseline Interferometry (VLBI) arrays, such as the East Asian VLBI Network (EAVN), Australia Long Baseline Array (LBA), and European VLBI Network (EVN) [31]. The antenna is an upgraded version of the Spanish Yebes radio telescope, working at 300 MHz-115 GHz [32].

2.1.10. Canadian Hydrogen Intensity Mapping Experiment Telescope. Canadian Hydrogen Intensity Mapping Experiment Telescope (CHIME) consists of four $20\,\text{m} \times 100\,\text{m}$ semicylindrical parabolic reflectors (Figure 11). It completed construction in September 2017 and began to operate for observation in September 2018. CHIME operates in the 400–800 MHz frequency band [33]. Each cylinder equipped with 256 dual-polarization feeds will continuously image the entire northern sky to measure the distribution of neutral hydrogen in the universe and study the properties of dark energy [34]. It is used to measure the expansion history of the universe by converting the collected cosmic signals into a three-dimensional map of hydrogen density [35]. CHIME could also be used to explore new fast radio bursts and pulsars [36].

2.1.11. Australian Square Kilometer Array Pathfinder. The Australian Square Kilometer Array Pathfinder (ASKAP) is a pioneer project of the first Square Kilometer Array (SKA) (Figure 12). It is located in the Murchison Radio

(a) (b)

Figure 2: Kashgar deep space station (https://www.sohu.com/a/273044755_772793 https://www.163.com/dy/article/FI7MU2RQ0512B07B.html).

Figure 3: Jiamusi deep space station (https://www.smoc.ac.cn/research/2318.jhtml).

Figure 4: Argentina deep space station. (https://cn.chinadaily.com.cn/a/202007/24/WS5f1a2d7fa310a859d09d9ca5.html).

Astronomy Observatory in Western Australia and has a total of 36 reflector antennas with a diameter of 12 m [37]. ASKAP began construction in 2009 and completed the deployment and assembly of all antennas by 2012 [38]. ASKAP's prototype is the Boolardy Engineering Test Array, the first aperture synthetic radio telescope to use phased array feed technology [39]. The success of early science projects using ASKAP could be seen in all areas of astrophysics, indicating that ASKAP's scientific prospects are very appealing [40].

2.1.12. Murchison Widefield Array. The Murchison Widefield Array (MWA), also located at the Murchison Radio Astronomy Observatory, is one of SKA's pioneering projects

Figure 5: Tianma 65 m radio telescope (http://radio.shao.cas.cn/).

(Figure 13). The first phase of the MWA was commissioned in 2013 and a total of 128 aperture arrays were constructed [41]. Then, it began the full operation. The second phase was completed in 2017 and officially put into use in 2018; the construction of the second phase doubled the number of antennas [42]. The MWA is an international effort by different countries and its data are publicly available [43]. MWA's primary scientific goals consist of four key scientific themes: searching for the redshift of 21 cm radiation in the reionization era of the early universe, galactic and extragalactic sky surveys, time-domain astrophysics, as well as the study of scientific problems and space weather in the sun, heliosphere, and ionosphere [44].

2.1.13. Karoo Array Telescope. The Karoo Array Telescope (MeerKAT) is a medium-sized pioneer telescope instrument group in SKA [45], located in South Africa, consisting of 197 offset reflector antennas with a diameter of 13.5 m (Figure 14). The concept of MeerKAT was first proposed in 2009 [46], and seven prototypes (KAT-7) were initially built [47]. It was not until January 2022 that the construction and networking of 197 antennas were finally completed [48]. After ten years of design and construction, the observation of the central region of the Milky Way has achieved promising results after MeerKAT was officially put into operation [49].

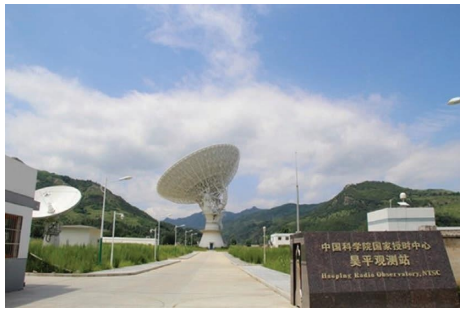

Figure 6: Haoping 40 m radio telescope (http://pic.cas.cn/pic_ntsc_cas/yqfm/201907/t20190709_5337491.html).

Figure 7: Wuqing 70 m radio telescope (https://www.sohu.com/a/480437535_162522).

Figure 8: FAST (https://www.sohu.com/a/115089151_116413).

2.1.14. Hydrogen Epoch of Reionization Array. The Hydrogen Epoch of Reionization Array (HERA) is located in the Karoo Radio Astronomy Reserve, South Africa. In 2016, 19 parabolic antennas with a diameter of 14 m were deployed (Figure 15). The HERA aims for a high-significance power spectrum measurement [50]. The main goal of HERA is to detect cosmic signals from the reionization era [51]. In the later stage, HERA will deploy a total of 350 antennas to form an array. At the same time, HERA is also the last of the four pioneer projects of SKA [52].

2.1.15. Low-Frequency Array. Low-Frequency Array (LOFAR) is a large distributed radio telescope (Figure 16) [53]. LOFAR was officially put into operation and

Figure 9: Greenland telescope (https://lweb.cfa.harvard.edu/greenland12m/pictures/).

Figure 10: Thai national radio telescope (https://spaceth.co/tnro/).

observation in December 2012, using the omnidirectional dipole antenna as the array element, working in the frequency band of 10 MHz to 240 MHz. Since it is a fixed antenna, LOFAR uses aperture synthesis software for imaging [54]. The lower operating frequency band of LOFAR enables it to greatly enhance the observation efficiency of pulsars in the low radio frequency band [55].

2.2. Radio Telescopes under Construction and Planning for Construction

2.2.1. QiTai 110 m Radio Telescope, Xinjiang, China. The ultra-large aperture fully steerable radio telescope QTT (QiTai Telescope) (Figure 17) is located in Qitai County, Xinjiang, China. Its aperture is as wide as 110 m, and its operating frequency covers 150 MHz-115 GHz, which is highly complementary to FAST [56]. The overall reflector surface structure of FAST is fixed on the ground, and the formation of the reflector surface needs to be controlled by the actuators during observation, while QTT can not only rotate in azimuth and pitch but also is equipped with the

Figure 11: Canadian hydrogen intensity mapping experiment telescope (https://nrc.canada.ca/en/research-development/nrc-facilities/dominion-radio-astrophysical-observatory-research-facility).

Figure 12: Australian square kilometer array pathfinder (https://www.csiro.au/en/news/News-releases/2021/In-the-blink-of-an-eye-astronomers-win-prestigious-American-science-prize).

Figure 13: Murchison widefield array (https://www.mwatelescope.org/).

active surface system, making it the largest single-dish fully steerable antenna in the world. The reflector adopts the shaping technology so that the main and secondary reflectors can be converted between the shaping and the standard surface to realize the focus multibeam. By using fast antenna measurement and shaping technology, the closed-loop control of the active surface is realized, and the deformation of the antenna mechanical structure caused by gravity and external load is corrected in time. The preresearch of QTT has also been carried out for nearly ten years. Recently, the Xinjiang Astronomical Observatory of the Chinese Academy of Sciences completed the bidding for the antenna construction at the end of September 2022. The construction period is expected to be 5 years. The completion of QTT will play an important role in the fundamental scientific research fields of gravitational wave detection, black hole discovery, and the origin of galaxies [11].

Figure 14: Karoo array telescope (https://africanews.space/a-commercially-driven-african-space-industry/).

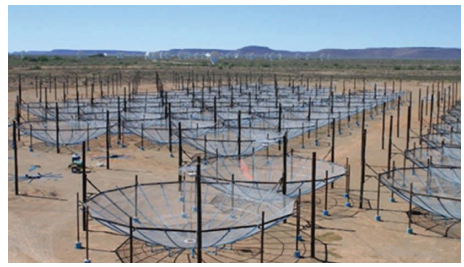

Figure 15: Hydrogen epoch of reionization array (https://caes.ukzn.ac.za/news/first-data-release-from-hera-team-gives-insight-into-the-early-universe/).

Figure 16: Low-frequency array (https://www.astron.nl/telescopes/lofar/).

2.2.2. Jingdong 120 m Radio Telescope, Yunnan, China. In August 2020, the Yunnan Provincial Government and the Chinese Academy of Sciences formally signed the "Cooperation Agreement on the Joint Construction of the Jingdong 120 m Pulsar Radio Telescope (JRT)" (Figure 18). In September, the project's launching ceremony was held in Jingdong, Pu'er City, Yunnan Province, marking the official start of construction of the world's largest omnidirectional rotatable low-frequency radio telescope. The construction period is expected to be three years [57]. The operating frequency of JRT is concentrated at 0.3–10 GHz, and the main observation target is pulsars. It will carry out cutting-edge scientific research such as gravitational wave detection and strong gravitational field relativity testing. Unlike QTT, which uses solid panels for the overall reflector surface, JRT only uses solid panels in the central 40 m diameter position, and mesh panels are used for the rest due to low-frequency operation and overall weight reduction.

Figure 17: Design sketch of QTT (https://baijiahao.baidu.com/s?id=1664409321011853698&wfr=spider&for=pc).

Figure 18: Design sketch of JRT (https://www.sohu.com/a/422487816_381442).

2.2.3. Shigatse and Changbaishan 40 m Radio Telescope, China. In the upcoming fourth phase of the lunar exploration mission, to meet the requirements of accurate VLBI orbit measurement, the Chinese Academy of Sciences plans to build two 40 m aperture radio telescopes measurement and control station in Shigatse, Tibet, and Changbaishan, Heilongjiang Province. Since 2018, the Shanghai Astronomical Observatory has traveled to Tibet seven times to investigate the site selection. Finally, the junction of Nie Rixiong Township, Sangzhuzi District, Shigatse City, and Chaxiu Township, Sakya County, was used as the construction site of the 40-meter radio telescope for the new lunar exploration project. In 2019, the Shanghai Astronomical Observatory (SOA) signed a cooperation agreement with the Shigatse City People's Government, which means that a new reflector antenna will be constructed in the central and southern parts of Tibet to help China Aerospace go further. Moreover, in 2021, the SOA also confirmed the construction site of the Changbaishan 40 m radio telescope and advanced the construction of the "six stations and one center" of the fourth phase of China's lunar exploration.

2.2.4. Nanjing Zijinshan Observatory 60 m Submillimeter Telescope. To promote China's submillimeter-wave astronomical observation capabilities, the Chinese astronomical community plans to build a 60 m aperture submillimeter-wave radio telescope, which is still in the preresearch and preparation stage. The plan is to develop submillimeter wave adaptive optics, manufacture phase reference artificially, use the phase reference transmitter of the main reflector to transmit microwave signals, observe with a scientific observation receiver, and correct the active surface in real time according to the real-time observation results, so as to realize the real-time measurement and correction of the antenna wavefront. In 2018, the Nanjing Zijinshan Observatory will take the lead to hold a seminar on key technologies for large-scale submillimeter-wave telescope antennas, and conduct technical exchanges and discussions on the design, construction, and operation of 60 m aperture submillimeter-wave telescope antennas.

2.2.5. Large Submillimeter Telescope in Japan. After the international astronomy community proposed the concept of the next-generation large-aperture single-dish telescope in 2008, the National Astronomical Observatory of Japan proposed the design concept of the Large Submillimeter Telescope (LST) in 2014 and published the first related paper in 2016 [58]. This telescope is expected to operate at 70–950 GHz. Its key technology is an active surface control technology. Each adjustable panel of the reflector can accurately compensate for gravity and thermal deformation and achieve high surface accuracy of each panel. The actuator on the back of the panel can adjust and correct the panel deformation in real time. LST was listed in 2020 as one of the large academic projects in the field of astronomy and astrophysics in the 2020 Master Plan by the Japan Science Council.

2.2.6. Atacama Large Aperture Submillimeter Telescope. The Atacama Large Aperture Submillimeter Telescope (AtLAST), which is expected to be built in Chile, is also a 50 m aperture reflector telescope that also works in the submillimeter wave band. Relative design concepts were proposed in 2015 [59], and more details were introduced in the AtLAST project in 2020 [60]. AtLAST uses an advanced cryogenic receiver, which is boxed in a cryogenic thermostat with a diameter of 1 m. The cryogenic thermostat is bolted to the ceiling of the equipment room at the focus of the reflector. It is obvious that the AtLAST project led by the European Union has the same aperture as the prementioned LST project, both working in the submillimeter wave band. Therefore, the Japanese Science Committee and the European Union are considering merging the two projects, which is expected to be completed in 2024 [61].

2.2.7. Cerro Chajnantor Atacama Telescope. The Cerro Chajnantor Atacama Telescope (CCAT), originally known as the Cornell Caltech Atacama Telescope, was designed jointly by Cornell University, Caltech, and the Jet Propulsion Laboratory. The three institutions jointly study the construction of a 25 m aperture submillimeter telescope on a 5000 m peak in northern Chile [62]. The antenna's back frame and main reflector will be constructed of carbon fiber reinforced plastic [63] as to meet the surface RMS error requirement of 10 microns [64]. However, due to the problem of funding, although the designing concept was proposed in 2006, the construction of the antenna has not yet started.

2.2.8. Lunar Crater Radio Telescope. The far side of the moon has an excellent environment for astronomical observation because the moon can act as a physical barrier to block signal interference from the Earth or the sun. In 2018, NASA proposed the construction of the Lunar Crater Radio Telescope (LCRT) [65], and by using the existing craters on the moon, crawling robots were used to arrange the wire mesh to form a parabolic reflector with a diameter of 1 km [66]. The telescope will work in the ultralow frequency range of 3–30 MHz [67], and the main scientific goal is to explore the evolution of the interstellar medium when the first stars in the universe were formed.

2.2.9. BINGO Radio Telescope. The Baryon acoustic oscillations from Integrated Neutral Gas Observations (BINGOs) project aim to build a radio telescope to detect baryon acoustic oscillations [68]. It will consist of two fixed 40 m aperture telescopes, equipped with a feed array with 50 receivers. The concept of the bingo project was proposed in 2012, and with the gradual progress of the project, the main structure of the telescope, the optical part, and the receiver prototype were completed around 2019, and the overall construction is expected to be completed around 2022 [69].

2.2.10. Hydrogen Intensity and Real-Time Analysis Experiment Radio Telescope. Hydrogen Intensity and Real-time Analysis eXperiment (HIRAX) is a radio telescope array located in Karoo, South Africa. It has the same working frequency and scientific goals as CHIME. CHIME is mainly used to detect the northern sky, while HIRAX is used to detect the southern sky [70]. They complement each other. HIRAX will consist of an array of 1024 6 m aperture reflector antennas [71]. A prototype array consisting of 8 antennas was first built in 2017 for preliminary experimental verification, and a pathfinder array with 128 antennas will be built in the future. It is expected to expand to the final 1024 antenna arrays in 2022 [72].

2.2.11. Square Kilometer Array. Square Kilometer Array (SKA) is a large-scale cooperation project between governments around the world. The related concept was first proposed in the early 1990s [73]. SKA is planned to be constructed in South Africa (mainly constructing mid-frequency arrays and dish arrays) and Australia (mainly constructing low-frequency arrays). After completion, it will have a total collecting area of more than 1 square kilometer. The approval for the start of construction from its governing Council occurred in June 2021 [74]. The large signal-collecting area makes it possess a high degree of sensitivity. Meanwhile, by using arrays composed of different antenna types (SKA low-frequency array: an array composed of dipole antennas, covering 50–350 MHz; SKA midfrequency array and SKA dish array: an array composed of 12 m or 15 m aperture antennas, covering 35 MHz–20 GHz), SKA can work in the ultrawide frequency band of 50 MHz–20 GHz.

2.3. Conclusion. It can be seen from the above development trends that in the field of radio astronomy, reflector antennas can achieve high bandwidth, high gain, and high resolution at low cost [75], thus becoming indispensable. At the same time, it is because of the higher and higher gain and resolution requirements that the antenna aperture is getting larger and larger, and the electromechanical coupling problem caused by the mutual influence and restriction between electrical properties and structure is also becoming increasingly prominent. Therefore, how to solve the problem of radio telescope in electromechanical coupling is crucial. The next section summarizes the research progress of key electromechanical coupling technologies in radio telescopes from the perspectives of design manufacturing and observation operating.

3. Research Progress of Electromechanical Coupling of Radio Telescopes

At this stage, the characteristics of various electromechanical coupling technologies can be summarized into three aspects, as shown in Figure 19. In terms of design and manufacture, electromechanical coupling modeling and design include theoretical models, environmental load characteristics analysis, antenna panel, and structure design and tolerance allocation of antenna morphology. In terms of observation operation, the antenna performance assurance under the two kinds of loads of slowly varying loads and rapidly varying loads is analyzed. This section introduces the development status of three aspects of electromechanical coupling technology around Figure 19 in detail.

3.1. Electromechanical Coupling Modeling and Design

3.1.1. Electromechanical Coupling Modeling. For large radio telescopes, Reference [76] point out that due to the large aperture of the reflector, the complex structure, and long-term working in the outdoor environment, environmental loads such as self-weight, sunshine, wind, and snow also cause negative effects. The systematic errors caused by these factors and the random errors generated during the installation and manufacture of the telescope will affect the ultimate performance of the telescope (such as pointing, gain, and others.). To accurately and quickly analyze the effects caused by these errors, it is necessary to develop an efficient and accurate computational tool [77], that is, the electromechanical coupling model of reflector antennas.

For the feedforward reflector antenna or double reflector antennas commonly used in engineering (the subreflector and feed can be equivalent to feed to the virtual focus of the subreflector by the equivalent feed method), Reference[78] points out that the main structural factors affecting electrical performance can be summarized into three aspects: main reflector error, feed pointing error, and feed position error. Therefore, the influence on the ideal pattern can be analyzed from these three aspects, and finally obtaining the electromechanical coupling model.

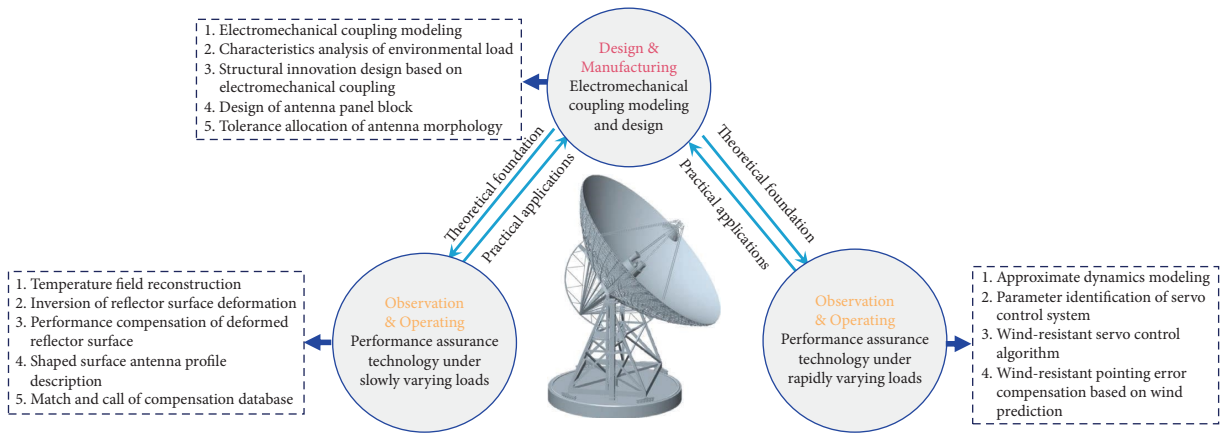

Figure 19: Electromechanical coupling technology for radio telescopes.

For the main reflector, its random errors can be described as different distribution functions on the main reflector, and then superimposed on the influence of systematic errors on the deformation of the reflector. The systematic error is a deterministic error, which can be obtained by finite element analysis. The main reflector area can be regarded as the far area of the feed. When the deformation of the main reflector is small (compared with the overall size of the antenna), the effect of the main surface error on the electromagnetic field amplitude of the aperture surface can be ignored, and it is considered that the main surface error will only cause relative errors on the electromagnetic field in the aperture surface [79, 80]. As for the feed source pointing error, that is, when there is an angular error between the feed source pointing and the central axis of the reflecting surface, the irradiation path from the feed source to the aperture surface will change, which will bring amplitude errors to the electromagnetic field of the aperture surface and will cause the sidelobe level to rise. For the feed position error, the offset of the feed position will change the phase center, thereby causing the phase change of the electromagnetic field of the aperture surface [78].

Combining the error effects of the previous three aspects and the ideal pattern formula of the reflector antenna, the final electromechanical coupling model of the reflector antenna can be obtained [81] as follows:

$$E(\theta,\phi) = \iint_A \frac{f_0\left(\xi - \Delta\xi(\delta(\beta)), \phi' - \Delta\phi'(\delta(\beta))\right)}{r_0} \cdot \exp j\left[k\rho' \sin\theta\cos\left(\phi - \phi'\right)\right]$$
$$\cdot \exp j\left[\varphi_f(\delta(\beta)) + \varphi_s(\delta(\beta)) + \varphi_r(\gamma)\right]\rho' \mathrm{d}\rho' \mathrm{d}\phi', \quad (1)$$

where $f_0(\xi - \Delta\xi(\delta(\beta)), \phi' - \Delta\phi'(\delta(\beta)))$ is the effect of the feed pointing error on the phase of the electromagnetic field on the aperture surface, $\varphi_f(\delta(\beta))$ is the effect of the feed position error on the electromagnetic field phase of the aperture surface, and $\varphi_s(\delta(\beta))$ and $\varphi_r(\gamma)$ are the main surface deformation and the effect of the main surface random error on the electromagnetic field phase of the aperture surface, respectively.

3.1.2. Characteristic Analysis of Environmental Load. After the electromechanical coupling model is established, to accurately analyze the effects of environmental loads in the designing phase (such as wind, temperature, and gravity), thereby giving an evaluation of the electric performance of the telescope's pointing gain, an accurate analysis of the influence mechanism of various environmental loads on the performance of the telescope is also of great necessity.

The wind in the natural environment can be divided into two types: steady-state winds and transient winds. The period of steady-state wind is generally much longer than the natural vibration period of the structure, and its influence on the structure can be regarded as a static force that does not change with time, thus applied to the structural for analysis as a static load. For instance, Reference [82] analyzes structural static deformation of the antenna under 8-level wind speed. Reference [83] analyzes wind pressure distribution on the reflecting surface of the antenna at a wind speed of 14 m/s through wind tunnel experiments. While the period of transient wind is short, its action properties are dynamic and will cause structural vibration. Structural vibration will lead to the change of the antenna pointing. Reference [84] analyzes the antenna vibration and pointing error changes under the influence of transient wind. For the larger aperture surface of the radio telescope, whether it is steady wind or transient wind, a certain torque will be generated on the antenna. Under the influence of this

torque, the antenna will undergo a certain torsional deformation, which will cause a change of the antenna pointing. References [85, 86] analyze the torque of the telescope antenna under wind load. Both thermal and gravitational loads can cause deformation of the reflector surface of the antenna, thereby affecting the final pointing and gain performance of the telescope. Any material will be deformed to a certain extent under an uneven temperature field. The telescope will be affected by the sun because it is always in the natural environment. The sun's irradiation will create a shadow area on the surface of the reflector surface and the back frame, which will cause the antenna to not be heated evenly, eventually causing the deformation of the reflector surface and the back frame. Reference [87] analyzes the thermal stress and deformation of the reflector surface of the antenna under different solar incident angles. Any substance will be affected by gravity, so the influence of gravity load is unavoidable, but since gravity will not change, as long as the attitude of the antenna does not change, then the gravitational deformation will not change, which can be analyzed by simulation or various measurement methods to obtain the deformation of the antenna under gravitational loads, such as total station [88], photogrammetry [89], and laser scanner [90].

3.1.3. Structural Innovation Design Based on Electromechanical Coupling. Although the influence of gravity load cannot be avoided, it can be reduced by means of structural conformal design [91]. The simplest and most effective way is to reduce the weight of the antenna back frame. However, if the weight of the back frame is reduced by simply reducing the number of trusses, it will inevitably lead to a reduction in the overall strength and stiffness of the antenna. On the premise of ensuring the rigidity and strength of the structure, replacing some truss structures with prestressed cables can not only reduce the weight of the antenna back frame but also change the stress distribution during the operation of the structure to reduce structural deformation [92]. Reference [93] uses parts of the tension and members of the antenna are replaced with prestressed cables. Under the same accuracy, the weight of the 8 m aperture reflector antenna is reduced by 15% through the cable-truss composite structure. In addition, the antenna structure can also be designed with equal flexibility, that is, it is necessary to optimize the topology of the antenna structure to ensure the consistency of its node deformation. Equal flexibility design can be seen in antennas such as 37 m HUSIR [94], 50 m LMT [95], 64 m SRT [96], and 110 m Effelsberg [97]. Meanwhile, Reference [98] also uses an equal flexibility design to optimize the support structure of the QTT 110 m antenna reflector that is to be constructed. The 16-point equal flexible support structure used in the support structure greatly improves the deformation of QTT.

For radio telescopes, the driving power required for the antenna base, whether it is a wheeled table or a roller type, is relatively large. No matter how the traditional optimization of the back frame or the base frame is carried out, the effect of reducing the weight of the antenna is not significant enough. Only by innovating the structure can the weight of the antenna be greatly reduced. Compared with the traditional series drive structure, the parallel drive structure has the advantages of high rigidity, high accuracy, large bearing capacity, and small motion load. For example, Reference [99] uses the 6-DOF Stewart platform to control the pointing of the AMiBA telescope. Among radio telescopes, the Stewart platform is mostly used to control the attitude of the subreflector and is not suitable for large antenna structures. In [100], the authors propose an innovative design of the antenna mechanism, including a cable-truss combined backup structure and parallel drive antenna, and used this design to verify the 26 m aperture antenna. The new design reduces the weight of the antenna by 54.3%, and the driving power is reduced by 63.3%.

3.1.4. Design of Antenna Panel Block. The ultimate purpose of the previously mentioned conformal design of the antenna structure is to ensure the surface accuracy of the telescope. With the increasing requirements for surface accuracy of large radio telescopes, the manufacturing accuracy of the antenna panel has become of vital significance. Considering the machining, transportation, installation, and manufacturing costs of the antenna, it is necessary to design a reasonable block of the main reflector panel of the antenna. The antenna panel is machined by molds. Therefore, although the smaller the panel, the higher the manufacturing accuracy; but the number of corresponding molds will also increase, thus increasing the cost. At the same time, the smaller the antenna panel, the more support structures are required for the overall installation of the antenna reflector, which will lead to increasingly complex back frame structures and increased self-weight. Therefore, the smaller antenna panel does not solve the problem and the mold of the antenna panel needs to be reasonably designed. For the QTT 110 m antenna, Reference [101] reduces the original 23 types of molds to 14 types of molds under the premise of meeting the requirements of the electrical performance of the antenna through reasonable block design and mold sharing strategy.

3.1.5. Tolerance Allocation of Antenna Morphology. The structural design of a radio telescope is a systematic project. Its structure consists of multiple substructures, such as wheel rails, mounts, back frames, feed bins, main reflectors, and subreflectors. These structures together determine the ideal performance of the telescope. In practical applications, the performance can also be controlled and compensated by the control system of the antenna. Reference [95] points out that the structural design of the antenna needs to find the optimal balance between structure and control because the final performance of the radio telescope is directly linked to the surface accuracy [102]. Meanwhile, the surface accuracy of the antenna is jointly determined by each substructure, which means that engineers need to reasonably allocate and control the tolerances of each substructure system. In the past, this process was usually performed by engineers using their own design experience. If the final performance did not meet the standard, then an adjustment was made and the

process is considered a trial error. After the electromechanical coupling model is established, the influence of each structural error on the final electrical performance can be analyzed through this model, to obtain the influence degree of each substructure of the antenna on the performance, and then allocate the tolerance accuracy more reasonably according to the influence degree. For example, Reference [103] analyzes the influence of axis errors such as the antenna azimuth axis and pitch axis and the orbital irregularity of the antenna wheel rail on the final pointing accuracy. Reference [104] lowers the accuracy requirements for the main reflector by using subreflector compensation technology, which can provide certain guidance for the tolerance allocation of the antenna's main surface panel in the design stage. Studies in References [79, 104] show that the accuracy of each ring panel on the main surface of the antenna has different effects on the final electrical performance. Together with Reference [101], it is explained that the accuracy of the panel near the center of the reflector has a greater impact on the electrical performance than that of the outer panel, so the machining accuracy of the inner panel can be improved during the process, and the machining of the outer panel can reduce its precision to a certain extent.

3.2. Performance Assurance Technology under Slowly Varying Loads

3.2.1. Temperature Field Reconstruction. Temperature load is one of the important loads of radio telescopes, and its most distinguishing feature is that it is greatly affected by sunlight. There are 2 methods to obtain the antenna temperature field distribution: finite element simulation and temperature sensor measurement. Finite element simulation is subject to the limitation of calculation speed and cannot guarantee the real-time acquisition of the temperature field. Due to the limitation of the structure of the antenna, engineers cannot put too many temperature sensors on the antenna for measurement. To ensure the accuracy and real-time performance of the antenna temperature field acquisition, it is necessary to accurately reconstruct the overall temperature field distribution of the antenna by using temperature data measured by a small number of temperature sensors through an appropriate method. Reference [105] combines two methods of sensor measurement and finite element simulation. Firstly, the temperature field database of the antenna at different times is obtained by using the finite element simulation analysis, and then the temperature field is obtained by looking up the measured temperature data in the database to obtain the overall temperature field distribution. Finally, the temperature field is corrected by the measured ambient temperature. An interpolation algorithm is used in [106] to interpolate the temperature data measured by a small number of sensors to obtain the overall temperature field distribution of the antenna.

3.2.2. Inversion of Reflector Surface Deformation. The reflector surface of the radio telescope will deform under the influence of gravity load and temperature load, in order to accurately analyze and compensate for the final performance of the telescope in real time (such as the need to quickly calculate the adjustment amount of the actuator, subreflector and feed source pointing, and others); it is of vital significance to quickly obtain the shape information of reflector surface. Reference [107] constructed influence factor matrix for fast calculation of thermal deformation of the antenna. Reference [108] uses precise diffraction algorithms to evaluate repetitive deformations of reflector surfaces. Reference [109] proposes a method for fast calculation of antenna panel deformation based on an angle sensor. Reference [110] proposes a method of fitting the reflector surface based on the least squares method. This method calculates the six key parameters required for the fitting equation of the reflector surface based on the principle of the least squares method and the integral extreme value theorem, and then obtains the fitting equation of the reflector surface and completing the reconstruction of the reflector surface.

3.2.3. Performance Compensation of Deformed Reflector Surface. When the main or subreflector of a radio telescope is deformed, it will cause problems such as reducing the antenna gain, elevating side lobes, and pointing deflection. Therefore, it is necessary to compensate for this part of the electrical performance loss through a certain compensation method, such as active surface adjustment, subreflector adjustment, or feed adjustment. Reference [81] shows that the gain loss is related to the RMS error of the reflector surface, so to compensate the gain, it is necessary to minimize the surface RMS error of the antenna. This is the purpose of the active surface adjustment technology. This technology actively adjusts the main reflector by installing actuators on the back of the antenna panel and uses the actuators to move the deformed panel to a specified position to reduce the surface RMS error. Active surface technology was proposed in the 1990s [111]. Until today, many large radio telescopes in the world have applied this technology. Reference [112] used active surface technology to effectively improve the observation efficiency of an antenna. Reference [76] proposes an active surface adjustment method based on electromechanical coupling theory. This method also uses the least squares principle to calculate the distance between the deformed surface and the optimal working surface and then outputs the distance information to the actuators to complete the active surface adjustment. Reference [113] used edge sensors to measure the deformation of the telescope and actuators to ensure the regular operation and high-quality data output of the radio telescope.

The subreflector adjustment refers to adjusting the subreflector of the antenna, such as subreflector pose adjustment, active subreflector adjustment, and array subreverse adjustment. The pose adjustment of the subreflector usually uses a Stewart platform with 6 degrees of freedom to adjust the overall position of the subreflector, so that the subreflector can better match the main reflector. For example, References [114, 115] describe in detail the Stewart system in the subreflector of the 26 m antenna in Nanshan,

Xinjiang, and the adjustment position of the subreflector is determined by maximizing the gain. The adjustment of the active subreflector is similar to the previously mentioned adjustment of the active surface, but the actuator is installed on the back of the subreflector. The electrical performance is compensated by adjusting the surface type of the subreflector surface. Active subreflector technology can be seen in radio telescopes such as the 43 m GreenBank Telescope [116], 37 m Haystack Telescope [117], and 100 m Effelsberg Telescope [118]. The adjustment of the array subreflector surface is essentially a kind of electronic compensation. The traditional subreflector surface is replaced by the array unit. By controlling the excitation amplitude and phase of each unit, a conjugate matching focal plane field is constructed. Thus, the isophase plane is achieved on the aperture plane. Reference [119] used the microstrip reflector array as a subreflector, the phase error of the aperture surface caused by the surface distortion of the main reflector is compensated, thereby significantly improving the antenna performance.

Feed adjustment is mainly divided into feed pose adjustment and array feed adjustment. In simple terms, the pose adjustment of the feed is to adjust the position and attitude of the feed to the theoretical position corresponding to the best-fit paraboloid focus, which is similar to subreflector pose adjustment. Reference [120] proposes a method to determine the adjustment amount of reflector antenna feed based on far-field information. Array feed adjustment is also a kind of electronic compensation technology. The array feed is used to replace the traditional waveguide feed, and the amplitude or phase of the received signal is changed by electrical modulation to achieve the antenna beamforming, to achieve compensation. References [121, 122] introduced a dual-polarized phased array feed with a low noise amplifier, which greatly improves the measurement speed of the antenna.

3.2.4. Shaped Surface Antenna Profile Description. In the application of reflector antennas, there is often a need for special beam coverage, or effective omnidirectional radiation power is required for the target area. At this time, the beam of the antenna needs to be shaped, and this type of antenna is called a shaped beam antenna or shaped surface antenna. The beamforming of the antenna can be realized by changing the antenna waveguide feeding device or the antenna surface structure. Thanks to the development of active surface technology, radio telescopes with the active surface system can achieve surface switching under the operating state of the antenna, to meet different observation requirements. Taking FAST as an example, FAST could be considered a special shaped surface antenna. The body of FAST is a spherical reflector with an aperture of 500 m. When observing, the position of the panels needs to be adjusted by the actuators so that some of its panels are combined into a paraboloid with an aperture of 300 m [123], which involves the conversion from spherical to parabolic. It can be seen that there are two technical contents in the process of switching the profile of the shaped surface: the profile description of the shaped surface antenna and the switching between the paraboloid and the shaped surface. Shaped surface antenna could be considered as a type of antenna with a special surface. There is no standard equation to describe the surface of this type of antenna. Therefore, the target surface needs to be described first when switching. Reference [124] uses the Jacobian polynomial to describe the surface of the shaped surface antenna, and the final surface description equation is obtained by using the particle swarm optimization algorithm. In [125], the geometric information of the antenna surface under the specified beam shape is obtained by using the geometrical optics method. In [126], a method of using Zernike polynomials to describe shaped surface antennas is proposed. The surface shape switching of the antenna is generally carried out under normal working conditions. It will be affected by external loads, which requires the calculation of the adjustment amount from the deformed surface to the target-shaped surface. The authors can adopt the idea of the optimal fitting surface and uses the least squares method to calculate the required displacement of each actuator node, thereby achieving the switching process from the deformed paraboloid to the shaped surface. The switching of the shaped surface to the paraboloid can be considered as an inverse process. First, the shaped surface and the best working surface (usually a paraboloid) are described, and then the nodes displacement between the shaped surface and the best working paraboloid is calculated, thereby achieving the switching process.

3.2.5. Match and Call of Compensation Database. During the operation of the radio telescope, there is often a real-time requirement for the compensation of electrical performance, to improve the observation efficiency. For the influence of slowly changing loads such as temperature load and gravity load, the finite element simulation clearly cannot meet the real-time requirement as the finite element model calculation is time-consuming. For gravity loads, the self-weight deformation of the antenna at any altitude can be obtained through advanced simulation. This is the same for temperature loads (as described in the first part of this section). When the deformation information is known, the corresponding adjustment amount can be calculated in advance as the adjustment amount can be directly matched and called by the look-up table method during the antenna observation process. In other words, the compensation amount can be quickly obtained by establishing a compensation database in advance. The key lies in the accuracy of database matches and calls. Reference [127] points out that the Italian 64 m SRT antenna stores the antenna compensation information corresponding to the self-weight deformation in the database in advance, and realizes real-time compensation by looking up the table during the operation of the antenna. Reference [128] uses the optimized best-fitting surface parameters and the matching degree of the main and auxiliary surfaces to call the adjustment value stored in the subreflector database in real time to compensate for the gravitational deformation of the main reflector. Reference [129] establishes a temperature database based on transient

temperature field simulation and then corrected the simulated temperature field extracted from the temperature database by using real-time measurement data and the look-up table method. Combined with the finite element model of the telescope, the thermal field can be calculated in real time and used for thermal deformation compensation. Reference [130] proposes a method for fast match and call of the compensated database, which guarantees the accuracy by matching the root mean square error, similarity regions, and critical regions of the data. Reference [131] used a thermal deformation database determined by numerical simulation according to the observation schedule in advance to compensate for thermal deformations in real-time.

3.3. Performance Assurance Technology under Rapidly Varying Loads

3.3.1. Approximate Dynamics Modeling. For radio telescopes in the natural environment, wind disturbance has become the most complex and difficult problem in various environmental loads due to its randomness and time variation. The wind load will not only cause the deformation of the antenna but also cause the vibration, resulting in unstable pointing and poor observation performance. Therefore, it is necessary to study how to prevent wind disturbance. To describe the pointing deviation caused by the deformation (flexibility and rigidity) of the reflector surface under disturbance, estimate the pointing direction of the telescope, and facilitate the design of a control system with good control performance, it is necessary to establish a high-precision dynamic model of the antenna structure. The dynamic modeling of the antenna could be established with theoretical modeling. Theoretical modeling can be divided into rigid modeling, flexible modeling, and rigid-flexible hybrid modeling. For example, Reference [132] used rigid modeling to model the 110 m GBT. The advantage is that the model order is small. However, with the increase of the antenna aperture, the flexible deformation of the antenna structure cannot be ignored. However, rigid modeling cannot reflect the antenna flexibility information; therefore the actual control effect of the designed controller is not so ideal. Reference [133] used flexible modeling to perform finite element analysis on large aperture antennas, which can estimate the structural deformation. Furthermore, it also carried out a modal analysis on the antenna based on finite element analysis, which can select the modal retention that has a greater impact on the antenna performance, carry modal polycondensation, reduce the degree of freedom, and combined it with the rigid body model to obtain the overall dynamics model of the antenna to facilitate the further design of the controller. Reference [134] establishes a dynamic model of the antenna structure based on the model superposition method, and the dynamic model is poly-condensed according to the influence degree of each vibration order on the pointing, and further established a rigid-flexible hybrid model. The established dynamic model of the large-scale reflector antenna for pointing control is not only beneficial to the design of the controller but also can reflect the influence of flexible deformation on the pointing.

3.3.2. Parameter Identification of Servo Control System. Large-scale radio telescopes are complex in structure, and due to the nonlinear effects such as wind load and friction, it is difficult to carry out accurate theoretical modeling. In this case, system modeling can be used to establish an accurate system model. The model uses the parameter identification algorithm to obtain important parameters that can characterize the behavior of the system, establish a model that can imitate the behavior of the real system, and use the current measurable system input and output to predict the future evolution of the system output, which is advantageous to the design of the controller. Classical system identification methods include the step response method, impulse response method, frequency response method, correlation analysis method, spectral analysis method, least square method, and maximum likelihood method. The parameter identification of a servo control system mainly includes two aspects, that is, the identification of parameters such as internal motor inductance and the identification of external mechanical parameters including load inertia, friction damping, and shaft stiffness. For example, Reference [135] used the method of online identification of the system to collect the input and output data of the control object in real time. The system mathematical model is established by using the fourth-order controlled autoregressive moving average model and selecting the quadratic index to perform least squares fitting on its parameters. Reference [133] presents the process of deriving the velocity loop model from field test data. It includes descriptions of antenna white noise testing, test conditions, input and output signals, open-loop testing, closed-loop testing, instrument setup, and system identification testing. The analytical context for data description and data processing is also included. Furthermore, the correlation between the antenna model and its elevated position and the diameter of the dish antenna is discussed, and finally the analytical model and the identification model are compared.

3.3.3. Wind-Resistant Servo Control Algorithm. For large-diameter and high-frequency antennas, the pointing error caused by wind disturbance is still one of the most difficult and insurmountable problems due to its randomness and time-varying. To improve the pointing accuracy of the antenna and effectively suppress the pointing error caused by wind disturbance, it is necessary to study the effective error analysis and control compensation method according to its characteristics, and design suitable servo control algorithms and servo control systems. For the LMT 50 m antenna, Reference [136] compares the antiwind disturbance capabilities of the antennas with four control algorithms, including PI-PI, PI-LQG, LQG-PID, and LQG-LQG algorithms, and the simulation results show that LQG-LQG has the best control effect. Reference [137] aims at the control method of radar antenna to suppress wind disturbance,

under the premise that the antenna is regarded as an ideal rigid model, the design of the controller is divided into two independent stages according to the design theory of disturbance observer and the principle of fuzzy control, that is, performance design phase and interference suppression phase. The results show that the fuzzy PID controller has better dynamic performance than the traditional PID controller, and the introduction of a disturbance observer can effectively reduce the pointing error caused by wind disturbance for the influence of wind load on pointing. Reference [138] deduced uncertain models suitable for different models for different types of beam waveguide antennas, and an H-infinity controller is designed in combination with the model. The results verify the effectiveness of the controller design method in suppressing wind disturbance in different antennas. The pointing performance based on the H-infinity controller is slightly better than the error compensation effect based on the LQG control. In addition, the frequency of gusts is much higher than the response frequency of the control system. When the wind direction and wind speed change, the control system has no time to adjust its control strategy, so the control system cannot compensate for the pointing error caused by wind disturbance effectively. Therefore, a threshold-based control strategy will be adopted in the future to be equivalent to the interference of the wind on the antenna for a period of time [7, 139]. In other words, for the wind over a period of time, an adjustment amount is used. In some long-term high wind fields, the active surface (under the threshold) and the servo dual-system control strategy can be used to achieve stable control.

3.3.4. Wind-Resistant Pointing Error Compensation Based on Wind Prediction. Wind disturbance has the characteristics of short-period pulsation, and the estimation process or measurement process of the measured wind has a time delay, which means that when the wind acts on the antenna reflector surface, the control system cannot make real-time adjustments according to the received interference signal. This requires reasonable prediction of incoming wind information and calculation of the adjustment amount in advance. An adjustment amount can be calculated at every moment, but it still takes time for the control system to act on the antenna to adjust. Therefore, it is necessary to calculate an optimal adjustment amount (threshold) for a certain period of time, and the antenna should be adjusted in advance to reduce the influence of wind disturbance. The establishment of the wind speed prediction model provides the possibility to compensate for the antenna pointing error in real time. Different from the traditional compensation strategy based on error feedback, predictive control is a state feedback compensation strategy that reduces future disturbances by generating compensation in advance. At the same time, it is a complex process to reduce the pointing error caused by the random wind disturbance throughout the antenna rotation angle generated by the compensation effect. To obtain the desired pointing performance, it is necessary to realize the matching between the compensation elements of each link. The specific manifestations are matching between prediction parameters and controller parameters (to realize the optimal selection of adaptive control parameters under variable-time forecast wind speed), matching between predicted values and performance (to avoid cumulative prediction errors introduced by predicted values), and time margin matching with system time delay (to avoid compensation lag caused by long-time iteration of complex control algorithm). Reference [140] verifies that it is possible to accurately estimate the radial and tangential velocity components of the wind field in a real-time manner, and verify the validity of the steady-state wind speed prediction model.

4. Conclusion and Future Challenges of Electromechanical Coupling

4.1. Conclusion. This paper takes several major radio astronomy discoveries in recent years as the starting point and shows the key role that radio telescopes play in these major discoveries. From the major VLBI networks, the authors can find a global development trend in radio telescopes. The guarantee and improvement of the performance of a single-dish radio telescope is the foundation of observation, and the network observation of radio telescopes between countries is also a method that can maximize the performance of telescopes. The authors then describe the development of radio telescopes built in the world in recent years and the development of telescopes or telescope arrays that are under construction or to be constructed. It can be seen that China has built a relatively large number of single-dish radio telescopes in recent years and has also actively participated in the construction of some international radio telescope arrays, such as the SKA. In Europe and the United States and other countries, the focus has been on the construction of telescope arrays in recent years. At the same time, single-dish antennas have been transformed, upgraded, and networked for observation.

Finally, the authors summarize the application of electromechanical coupling technology in radio telescope design and challenges from three perspectives of electromechanical coupling modeling and design, performance assurance technology under slowly varying loads, and performance assurance technology under rapidly varying loads.

4.2. Future Challenges of Electromechanical Coupling. In future, with the development of radio telescopes in the direction of higher apertures or higher frequency bands, the author believes that the following technical challenges should be addressed.

4.2.1. Uncertainty Analysis and Processing of Radio Telescope Errors. For electronic equipment with integrated structure and function as a radio telescope, the mechanical structure is the carrier of its electrical performance, the device performance is the guarantee of its electrical performance improvement, the material parameters are the constraints of its electrical performance breakthrough, and the environmental

factors are obstacles to the stability of its electrical properties. With the development of radio telescopes in the direction of high frequency and high gain, the influence of the above four factors on performance is becoming increasingly obvious, and there is still a phenomenon of mutual coupling between these four aspects. At the same time, in engineering, there are uncertain factors such as manufacturing and installation errors, device performance temperature drift, material parameter changes, and environmental load fluctuations. If these uncertain factors are treated as deterministic information, this might lead to contradictory or very unreasonable results. Thus, in the follow-up research process, a certain uncertainty analysis method can be used for the error. On the basis of sorting out the influence mechanism of uncertainty factors on the telescope, a coupling model and performance guarantee methods that are more in line with the actual situation are proposed.

4.2.2. Wind Regulation Technology for Large Radio Telescope. Most of the existing radio telescopes use passive methods such as wind resistance control or the construction of a radome to reduce the impact of natural wind. Wind resistance control is likely to be ineffective in the high-frequency wind or strong wind conditions. The radome is expensive to build and affects the electrical performance, making it impractical for large radio telescopes. Thus, the authors need to start from another point of view to weaken the influence of wind by actively reducing the wind speed or changing the wind direction, which is called wind regulation technology. Wind regulation is to design of a wind regulation device by using the topographic and geomorphological features of the telescope site without changing the state of the telescope to achieve the purpose of actively reducing the near-field wind speed of the antenna and guiding the wind flow to bypass the antenna, thereby reducing the wind disturbance of the radio telescope and increasing the high-frequency stable observation time of the telescope. The idea of wind field regulation is to weaken the wind energy, reduce wind speed, and change the wind direction to achieve the effect of stabilizing observation and increasing operation time. The difficulty of regulation lies in how to regulate the wind at a height of 100 meters. On the one hand, the focus of wind field regulation is to design the device structure with a good shading effect and great consumption of wind energy. On the other hand, it is the synergy with terrain-based wind prediction and antenna servo system compensation.

4.2.3. Application of Low-Cost New Materials in Antenna Structure Design. At present, radio telescopes basically use metal materials to build the mechanical structure of the antenna. The high density of the metal material itself leads to a large self-weight of the antenna, and there is a natural structural limit. New materials could be used to design the structure of telescopes. Because of its excellent mechanical properties, carbon fiber composite material is a composite material with resin as the matrix and carbon fiber as reinforcement. It has the characteristics of lightweight, high modulus, and low thermal expansion coefficient. At the same time, this material itself has electrical conductivity, so the antenna made of carbon fiber composite material can not only ensure the electrical performance of the antenna, but also light in weight, strong in shock and vibration resistance, and can withstand harsh environments such as high and low temperature, thermal vacuum, and others. Carbon fiber-reinforced resin composite materials have the characteristics of low expansion, lightweight, and high strength. For high-precision antennas serving in extreme site environments, carbon fiber composite materials are very ideal reflector materials. The surface of carbon fiber composites needs to be coated with metal coatings by magnetron sputtering to achieve an efficient reflection of electromagnetic waves. On top of the metal coating, the magnetron sputtering method is used to coat the dielectric layer to protect the metal layer, which not only plays the role of antioxidation and anticorrosion but also ensures the thermal performance of the reflective surface during operation. Epoxy resin coating is currently the most widely used, but the anticorrosion ability of pure epoxy resin is limited. Adding fillers to epoxy resin coatings to prepare epoxy resin-based composite anticorrosion coatings is an effective way to improve the anticorrosion ability of epoxy resin coatings. Silicon nitride has a low dielectric constant and dielectric loss, as well as a series of excellent properties such as high strength, high hardness, electrical insulation, thermal shock resistance, corrosion resistance, and wear resistance and is recognized as the most promising new wave-transmitting material. The previously mentioned new materials have broad application prospects in radio telescopes, but due to factors such as cost, they are rarely used in antennas at this stage.

4.2.4. Performance Assurance Technology under the Simultaneous Action of Transient Wind and Temperature Loads. Due to its special outdoor working environment, large-aperture radio telescopes are inevitably affected by external loads such as gravity, temperature, and wind loads. The influence of these three loads on the surface accuracy of the reflector and the electrical performance has been analyzed in the previous section separately, but the actual service environment of the antenna cannot have only a single load. For example, the temperature uniformity of the reflective surface will affect its structural deformation due to the action of the wind field. Therefore, the influence mechanism of the unsteady wind and temperature fields on the electrical performance of large antennas should be studied in the future.

4.2.5. Moon-Based Radio Telescope. The aperture of the radio telescope on the Earth has reached its limit due to the influence of gravity. The gravity on the moon is only 1/6 of that on the Earth. Naturally, it is possible to consider establishing a radio telescope with a large aperture (120 m and above) on the moon, for example, the Lunar Crater Radio Telescope mentioned earlier in this article. However, the telescope is a mesh antenna, and it can only perform low-frequency observations after completion. If high-frequency signals are to be received, then a solid panel must be used to build the antenna. In 2021, China and Russia jointly issued

the Joint Statement of the China National Space Administration and Roscosmos on Cooperation in the Construction of an International Lunar Research Station. This means that China and Russia will work with other international partners to jointly build an international lunar scientific research station, of which the lunar astronomical observatory is one of the key points. Therefore, it is foreseeable that the moon-based radio telescope will be a major research hotspot in the future. Among them, lunar morphology analysis, telescope selection, energy supply, environmental protection technology, thermal control technologies (heat dissipation on lunar day and heat preservation on lunar night), assembly, measurement and commissioning calibration, telescope operation and maintenance, and remote monitoring will all be areas for breakthroughs.

Data Availability

The data used to support the findings of this study are available from the corresponding author upon reasonable request.

Conflicts of Interest

The authors declare that they have no conflicts of interest regarding the publication of this paper.

Acknowledgments

This work was supported by the National Key Research and Development Program of China under grant no. 2021YFC2203600, National Natural Science Foundation of China under grant nos. 52005377 and 51975447, and Youth Innovation Team of Shaanxi Universities under grant no. 201926.

References

[1] R. Cowen, "Telescope captures view of gravitational waves," *Nature*, vol. 507, no. 7492, pp. 281–283, 2014.

[2] X. Li, "Primordial gravitational waves," *Science*, vol. 66, no. 3, pp. 16–20, 2014, in Chinese.

[3] A. J. Levan and P. G. Jonker, "Electromagnetic counterparts of gravitational wave sources at the Very Large Telescope," *Nature Reviews Physics*, vol. 2, no. 9, pp. 455–457, 2020.

[4] K. Akiyama, A. Alberdi, W. Alef et al., "First M87 event horizon telescope results. II. Array and instrumentation," *The Astrophysical Journal Letters*, vol. 875, no. 1, p. L2, 2019.

[5] B. Marcote, K. Nimmo, J. W. T. Hessels et al., "A repeating fast radio burst source localized to a nearby spiral galaxy," *Nature*, vol. 577, no. 7789, pp. 190–194, 2020.

[6] Y. Rahmat-Samii and R. Haupt, "Reflector antenna developments: a perspective on the past, present and future," *IEEE Antennas and Propagation Magazine*, vol. 57, no. 2, pp. 85–95, 2015.

[7] C. Wang, L. Xiao, B. Xiang et al., "Development of active surface technology of large radio telescope antennas," *Sci Sin-Phys Mech Astron*, vol. 47, no. 5, in Chinese, Article ID 059503, 2017.

[8] B. Duan, *Theory, Methods and Applications of Electromechanical Coupling in Electronic Equipment*, Peiking:Science Press, Beijing, China, 2011, in Chinese.

[9] B. Du, Y. Wu, Y. Zhang et al., "Overview of large reflector antenna technology," *Radio and Communications Technology*, vol. 42, no. 1, pp. 1–8, 2016, in Chinese.

[10] S. von Hoerner and W.-Y. Wong, "Gravitational deformation and astigmatism of tiltable radio telescopes," *IEEE Transactions on Antennas and Propagation*, vol. 23, no. 5, pp. 689–695, 1975.

[11] N. Wang, "Xinjiang Qitai 110 m radio telescope," *Sci Sin-Phys Mech Astron*, vol. 44, no. 8, pp. 783–794, 2014, in Chinese.

[12] W. Wu, H. Li, and Z. Li, "Status and prospect of China's deep space TT&C network," *Sci Sin Inform*, vol. 50, no. 1, pp. 93–114, 2020, in Chinese.

[13] G. Yu, J. Liu, and L. Zhang, "The "Chang'e" 4 relay star "Queqiao" to build the Earth-Moon communication link," *Aerospace China*, vol. 1, pp. 19–23, 2019, in Chinese.

[14] Y. Yu, L. Han, S. Zhou et al., "A study on the measurements and improvements of pointing accuracy of Jiamusi 66 m radio telescope," *Astronomical Research & Technology*, vol. 13, no. 4, pp. 408–415, 2016, in Chinese.

[15] G. He, M. Liu, X. Gao, X. Du, H. Zhou, and H Zhu, "Chinese deep space stations: a brief review [antenna applications corner]," *IEEE Antennas and Propagation Magazine*, vol. 64, no. 1, pp. 102–111, 2022.

[16] G. Dong, H. Li, W. Han et al., "Development and future of China's deep space TT&C system," *Journal of Deep Space Exploration*, vol. 5, no. 2, pp. 99–114, 2018, in Chinese.

[17] Z. Shen, "Progress in the development and scientific observation of the Tianma Telescope," in *Proceedings of the Chinese Astronomical Society Annual Academic Conference*, Paris, France, July 2017, in Chinese.

[18] Q. Liu, Q. He, X. Zheng et al., "Analysis of VLBI observation for Tianma radio telescope in Chang'E-3 orbit determination," *Sci Sin-Phys Mech Astron*, vol. 3, pp. 83–91, 2015, in Chinese.

[19] H. Qian, Y. Liu, F. Fan et al., "Analysis of surface shape accuracy of main reflector of 65m antenna structure," *Infrared and Laser Engineering*, vol. 41, no. 11, pp. 3027–3033, 2012, in Chinese.

[20] Z. Tian, "Precision determination of phase center coordinates of 40 m aperture radio antenna at Haoping Station of National Time Service Center," in *Proceedings of the Chinese Astronomical Society Annual Academic Conference*, Beijing, China, April 2015, in Chinese.

[21] J. Luo, Y. Gao, T. Yang et al., "Pulsar timing observations with haoping radio telescope," *Research in Astronomy and Astrophysics*, vol. 20, no. 7, p. 111, 2020.

[22] J. Luo, "40m aperture radio telescope of national time service center of Chinese Academy of sciences," in *Proceedings of the Chinese Astronomical Society Annual Academic Conference*, Antalya, Turkey, Sptember 2017, in Chinese.

[23] M. Zhang, H. Wang, Y. Zuo et al., "A review of the technical development of the structures of radio telescopes," *Journal of Huazhong University of Science and Technology*, vol. 1, 12 pages, 2022, in Chinese.

[24] D. Q. Kong, C. L. Li, H. B. Zhang et al., "The new wuqing 70 m radio telescope and measurements of main electronic properties in the X-band," *Research in Astronomy and Astrophysics*, vol. 22, no. 3, Article ID 035013, 2022.

[25] R. Nan, "FAST--500 meter aperture spherical telescope," *Chinese National Astronomy*, vol. 11, pp. 16–23, 2009, in Chinese.

[26] J. Yan and H. Zhang, "Introduction to main application goals of five-hundred-meter aperture spherical radio telescope," *Journal of Deep Space Exploration*, vol. 2, pp. 128–135, 2020, in Chinese.

[27] R. Nan, Di Li, C. Jin et al., "The five-hundred-meter aperture spherical radio telescope (FAST) project," *International Journal of Modern Physics D*, vol. 20, no. 6, pp. 989–1024, 2011.

[28] P. Raffin, J. C. Algaba-Marcosa, K. Asada et al., "The Greenland Telescope (GLT): antenna status and future plans," *Ground-based and Airborne Telescopes V*, International Society for Optics and Photonics, vol. 9145, Article ID 91450G, 2014.

[29] M. Inoue, J. C. Algaba-Marcos, K. Asada et al., "Greenland telescope project: direct confirmation of black hole with sub millimeter VLBI," *Radio Science*, vol. 49, no. 7, pp. 564–571, 2014.

[30] M. T. Chen, P. Raffin, P. T. P. Ho et al., "The Greenland telescope: thule operations," *Ground-based and Airborne Telescopes VII*, International Society for Optics and Photonics, vol. 10700, Article ID 107000H, 2018.

[31] P. Jaroenjittichai, K. Sugiyama, B. H. Kramer et al., "Sciences with Thai national radio telescope," 2022, https://arxiv.org/abs/2210.04926arXiv preprint arXiv:2210.04926.

[32] P. Jaroenjittichai, K. Bandudej, and P. Kempet, "Radio astronomy network and geodesy for development project: the 40-m Thai national radio telescope," in *Proceedings of the 2017 International Symposium on Antennas and Propagation (ISAP)*, pp. 1-2, IEEE, London, UK, December 2017.

[33] M. Amiri, K. Bandura, A. Boskovic et al., "An overview of CHIME, the Canadian hydrogen intensity mapping experiment," *The Astrophysical Journal - Supplement Series*, vol. 261, no. 2, p. 29, 2022.

[34] K. Bandura, A. N. Bender, J. F. Cliche et al., "ICE: a scalable, low-cost FPGA-based telescope signal processing and networking system," *Journal of Astronomical Instrumentation*, vol. 05, no. 04, Article ID 1641005, 2016.

[35] L. B. Newburgh, G. E. Addison, M. Amiri et al., "Calibrating CHIME: a new radio interferometer to probe dark energy," *Ground-based and Airborne Telescopes V*, International Society for Optics and Photonics, vol. 9145, Article ID 91454V, 2014.

[36] M. Amiri, K. Bandura, P. Berger et al., "The CHIME fast radio burst project: system overview," *The Astrophysical Journal*, vol. 863, no. 1, p. 48, 2018.

[37] S. Johnston, R. Taylor, M. Bailes et al., "Science with ASKAP," *Experimental Astronomy*, vol. 22, no. 3, pp. 151–273, 2008.

[38] J. M. Dickey, N. McClure-Griffiths, S. J. Gibson et al., "GASKAP—the galactic ASKAP survey," *Publications of the Astronomical Society of Australia*, vol. 30, 2013.

[39] D. McConnell, J. R. Allison, K. Bannister et al., "The Australian square kilometre array pathfinder: performance of the Boolardy engineering test array," *Publications of the Astronomical Society of Australia*, vol. 33, 2016.

[40] K. Lee-Waddell, "Early science results from ASKAP," in *Proceedings of the 2017 XXXIInd General Assembly and Scientific Symposium of the International Union of Radio Science (URSI GASS)*, pp. 1–4, IEEE, Montreal, QC, Canada, August 2017.

[41] S. J. Tingay, R. Goeke, J. D. Bowman et al., "The Murchison widefield array: the square kilometre array precursor at low radio frequencies," *Publications of the Astronomical Society of Australia*, vol. 30, 2013.

[42] R. B. Wayth, S. J. Tingay, C. M. Trott et al., "The phase ii murchison widefield array: design overview," *Publications of the Astronomical Society of Australia*, vol. 35, 2018.

[43] S. Prabu, P. Hancock, X. Zhang et al., "Improved sensitivity for space domain awareness observations with the murchison widefield array," *Advances in Space Research*, vol. 70, no. 3, pp. 812–824, 2022.

[44] J. D. Bowman, I. Cairns, D. L. Kaplan et al., "Science with the murchison widefield array," *Publications of the Astronomical Society of Australia*, vol. 30, 2013.

[45] R. S. Booth and J. L. Jonas, "An overview of the MeerKAT project," *African Skies*, vol. 16, p. 101, 2012.

[46] J. L. Jonas, "MeerKAT—the South African array with composite dishes and wide-band single pixel feeds," *Proceedings of the IEEE*, vol. 97, no. 8, pp. 1522–1530, 2009.

[47] P. G. Wiid, H. C. Reader, and R. H. Geschke, *Karoo Array Telescope: Lightning protection Issues and RFI[C]//2011 XXXth URSI General Assembly and Scientific Symposium*, pp. 1–4, IEEE, 2011.

[48] G. P. Swart, P. E. Dewdney, and A. Cremonini, "Highlights of the SKA1-Mid telescope architecture," *Journal of Astronomical Telescopes, Instruments, and Systems*, vol. 8, no. 01, Article ID 011021, 2022.

[49] I. Heywood, F. Camilo, W. D. Cotton et al., "Inflation of 430-parsec bipolar radio bubbles in the Galactic Centre by an energetic event," *Nature*, vol. 573, no. 7773, pp. 235–237, 2019.

[50] D. Jacobs, "HERA collaboration. Phase 1 results from HERA, the hydrogen epoch of reionization array," *American Astronomical Society Meeting Abstracts*, vol. 54, no. 6, pp. 314–407, 2022.

[51] A. R. Neben, R. F. Bradley, J. N. Hewitt et al., "The hydrogen epoch of reionization array dish. I. Beam pattern measurements and science implications," *The Astrophysical Journal*, vol. 826, no. 2, p. 199, 2016.

[52] D. R. DeBoer, A. R. Parsons, J. E. Aguirre et al., "Hydrogen epoch of reionization array (HERA)," *Publications of the Astronomical Society of the Pacific*, vol. 129, no. 974, Article ID 045001, 2017.

[53] M. de Vos, A. W. Gunst, and R. Nijboer, "The LOFAR telescope: system Architecture and signal processing," *Proceedings of the IEEE*, vol. 97, no. 8, pp. 1431–1437, 2009.

[54] M. P. van Haarlem, M. W. Wise, A. W. Gunst et al., "LOFAR: the low-frequency array," *Astronomy and Astrophysics*, vol. 556, p. A2, 2013.

[55] B. W. Stappers, J. W. T. Hessels, A. Alexov et al., "Observing pulsars and fast transients with LOFAR," *Astronomy and Astrophysics*, vol. 530, p. A80, 2011.

[56] K. J. Lee, J. P. Yuan, J. B. Wang et al., "The potential breakthroughs of GW detection using future Chinese radio telescopes," *Sci Sin-Phys Mech Astron*, vol. 47, no. 5, pp. 61–66, 2017, in Chinese.

[57] H. Zhang, Q. Huang, and Q. Shi, "Exploring the mystery of the shy-- Important instruments for astronomy and science in Yunnan," *Yunnan Science and Technology Management*, vol. 6, p. 2, 2020, in Chinese.

[58] R. Kawabe, K. Kohno, Y. Tamura et al., "New 50-m-class single-dish telescope: large submillimeter telescope (LST)," *Ground-based and Airborne Telescopes VI*, International Society for Optics and Photonics, vol. 9906, Article ID 990626, 2016.

[59] M. R. Bolcar, K. Balasubramanian, M. Clampin et al., "Technology development for the advanced technology large aperture space telescope (ATLAST) as a candidate large UV-

optical-infrared (LUVOIR) surveyor," *UV/Optical/IR Space Telescopes and Instruments: Innovative Technologies and Concepts VII*, International Society for Optics and Photonics, vol. 9602, Article ID 960209, 2015.

[60] P. D. Klaassen, T. K. Mroczkowski, C. Cicone et al., "The Atacama large aperture submillimeter telescope (AtLAST)," *Ground-based and Airborne Telescopes VIII*, International Society for Optics and Photonics, vol. 11445, Article ID 114452F, 2020.

[61] K. Kohno, R. Kawabe, Y. Tamura et al., "Large format imaging spectrograph for the large submillimeter telescope (LST)," *Millimeter, Submillimeter, and Far-Infrared Detectors and Instrumentation for Astronomy X*, International Society for Optics and Photonics, vol. 11453, Article ID 114530N, 2020.

[62] T. A. Sebring, R. Giovanelli, S. Radford et al., "Cornell Caltech Atacama telescope (CCAT): a 25-m aperture telescope above 5000-m altitude," *Ground-based and Airborne Telescopes*, International Society for Optics and Photonics, vol. 6267, Article ID 62672C, 2006.

[63] D. P. Woody, S. Padin, and T. Sebring, "CFRP truss for the CCAT 25m diameter submillimeter-wave telescope," *Ground-based and Airborne Telescopes III*, International Society for Optics and Photonics, vol. 7733, Article ID 77332B, 2010.

[64] D. Woody, S. Padin, E. Chauvin et al., "The CCAT 25m diameter submillimeter-wave telescope," *Ground-based and Airborne Telescopes IV*, International Society for Optics and Photonics, vol. 8444, Article ID 84442M, 2012.

[65] S. Bandyopadhyay, J. Lazio, A. Stoica et al., "Conceptual ideas for radio telescope on the far side of the Moon," in *Proceedings of the 2018 IEEE Aerospace Conference*, pp. 1–10, IEEE, Big Sky, MT, USA, March 2018.

[66] S. Bandyopadhyay, P. Mcgarey, A. Goel et al., "Conceptual design of the Lunar Crater Radio telescope (LCRT) on the far side of the moon," *IEEE*, in *Proceedings of the 2021 IEEE Aerospace Conference (50100)*, pp. 1–25, Big Sky, MT, USA, March 2021.

[67] G. Gupta, M. Arya, A. Goel et al., "Detector development for the Lunar Crater Radio telescope," *IEEE*, in *Proceedings of the 2022 IEEE Wireless Antenna and Microwave Symposium (WAMS)*, pp. 1–5, Rourkela, India, June 2022.

[68] C. A. Wuensche, "The BINGO telescope: a new instrument exploring the new 21 cm cosmology window," *Journal of Physics: Conference Series*, vol. 1269, no. 1, Article ID 012002, 2019.

[69] E. Abdalla, E. G. M. Ferreira, R. G. Landim et al., "The BINGO project I: baryon acoustic oscillations from integrated neutral Gas observations," 2021, https://arxiv.org/abs/2107.01633arXiv preprint arXiv:2107.01633.

[70] B. Saliwanchik, K. Bandura, H. C. Chiang et al., "Mechanical and optical design of the HIRAX radio telescope," *Ground-based and Airborne Telescopes VIII*, vol. 11445, Article ID 114455O, 2020.

[71] L. B. Newburgh, K. Bandura, M. A. Bucher et al., "HIRAX: a probe of dark energy and radio transients," *Ground-based and Airborne Telescopes VI*, International Society for Optics and Photonics, vol. 9906, Article ID 99065X, 2016.

[72] E. R. Kuhn, B. R. B. Saliwanchik, M. Harris et al., "Noise temperature testing for the hydrogen intensity and real-time analysis eXperiment (HIRAX)," *Ground-based and Airborne Telescopes VIII*, International Society for Optics and Photonics, vol. 11445, Article ID 114452Z, 2020.

[73] P. Hall, R. Schillizzi, P. Dewdney et al., "The square kilometer array (SKA) radio telescope: progress and technical directions," *International Union of Radio Science URSI*, vol. 236, pp. 4–19, 2008.

[74] J. McMullin, P. Diamond, M. Caiazzo et al., "The square kilometre array project update," *Ground-based and Airborne Telescopes IX. SPIE*, vol. 12182, pp. 263–271, 2022.

[75] Y. Rahmat-Samii and A. Densmore, "A history of reflector antenna development: past, present and future," in *Proceedings of the 2009 SBMO/IEEE MTT-S International Microwave and Optoelectronics Conference (IMOC)*, pp. 17–23, IEEE, Belem, Brazil, November 2009.

[76] C. S. Wang, L. Xiao, W. Wang et al., "An adjustment method for active reflector of large high-frequency antennas considering gain and boresight," *Research in Astronomy and Astrophysics*, vol. 17, no. 5, p. 043, 2017.

[77] B. Y. Duan and C. S. Wang, "Reflector antenna distortion analysis using MEFCM," *IEEE Transactions on Antennas and Propagation*, vol. 57, no. 10, pp. 3409–3413, 2009.

[78] L. Song, B. Duan, and F. Zheng, "Effects of reflector errors and phase center errors of feed on the far-field pattern of reflector antennas," *Systems Engineering and Electronics*, vol. 6, p. 6, 2009, in Chinese.

[79] Y. Rahmat-Samii, "An efficient computational method for characterizing the effects of random surface errors on the average power pattern of reflectors," *IEEE Transactions on Antennas and Propagation*, vol. 31, no. 1, pp. 92–98, 1983.

[80] L. Song, B. Duan, F. Zheng et al., "The effect of surface error on reflector antenna performance," *Acta Electronica Sinica*, vol. 37, no. 3, pp. 552–556, 2009, in Chinese.

[81] C. Wang, W. Wang, and L. Song, *Microwave Antenna Multi-Field Coupling Theory and Technology [M]*, Science Press, 2015, in Chinese.

[82] Q. Huang, X. Qin, and H. Huang, "Analysis of stress and strain on radar antenna based on wind loads," *Modern Radar*, vol. 29, no. 11, p. 4, 2007, in Chinese.

[83] Y. Liu, H. L. Qian, and F. Fan, "Reflector wind load characteristics of the large all-movable antenna and its effect on reflector surface precision," *Advanced Steel Construction: International Journal*, vol. 13, no. 1, pp. 1–29, 2017.

[84] W. Liang, J. Huang, and J. Zhang, "A new adaptive system for suppression of transient wind disturbance in large antennas," *International Journal of Antennas and Propagation*, vol. 2019, Article ID 2015341, 13 pages, 2019.

[85] W. Gawronski, "Modeling wind-gust disturbances for the analysis of antenna pointing accuracy," *IEEE Antennas and Propagation Magazine*, vol. 46, no. 1, pp. 50–58, 2004.

[86] W. Gawronski, J. A. Mellstrom, and B. Bienkiewicz, "Antenna mean wind torques: a comparison of field and wind-tunnel data," *IEEE Antennas and Propagation Magazine*, vol. 47, no. 5, pp. 55–59, 2005.

[87] C. S. Wang, S. Yuan, X. Liu et al., "Temperature distribution and influence mechanism on large reflector antennas under solar radiation," *Radio Science*, vol. 52, no. 10, pp. 1253–1260, 2017.

[88] M. Brenner, M. J. Britcliffe, and W. A. Imbriale, "Gravity deformation measurements of 70 m reflector surfaces," *IEEE Antennas and Propagation Magazine*, vol. 44, no. 6, pp. 187–192, 2002.

[89] R. Subrahmanyan, "Photogrammetric measurement of the gravity deformation in a Cassegrain antenna," *IEEE Transactions on Antennas and Propagation*, vol. 53, no. 8, pp. 2590–2596, 2005.

[90] P. Sarti, L. Vittuari, and C. Abbondanza, "Laser scanner and terrestrial surveying applied to gravitational deformation monitoring of large VLBI telescopes' primary reflector," *Journal of Surveying Engineering*, vol. 135, no. 4, pp. 136–148, 2009.

[91] S. von Hoerner, "Design of large steerable antennas," *The Astronomical Journal*, vol. 72, p. 35, 1967.

[92] G. Greschik, "Truss beam with tendon diagonals: mechanics and designs," *AIAA Journal*, vol. 46, no. 3, pp. 557–567, 2008.

[93] S. Feng, B. Duan, C. Wang, X. Duan, W. Wang, and Y Ban, "Topology optimization of pretensioned reflector antennas with unified cable-bar model," *Acta Astronautica*, vol. 152, pp. 872–879, 2018.

[94] R. P. Ingalls, J. Antebi, J. A. Ball et al., "Upgrading the Haystack radio telescope for operation at 115 GHz," *Proceedings of the IEEE*, vol. 82, no. 5, pp. 742–755, 1994.

[95] H. J. Kärcher and J. W. M. Baars, "Design of the large millimeter telescope/gran telescopio millimetrico (LMT/GTM)[C]//Radio Telescopes," *International Society for Optics and Photonics*, vol. 4015, pp. 155–168, 2000.

[96] H. J. Kärcher, "Telescope structures worldwide," *Steel Construction*, vol. 2, no. 3, pp. 149–160, 2009.

[97] J. Mar and H. Liebowitz, "The 100-m radio telescope of the max planck Institute for radio astronomy in bonn," *Structures Technology for Large Radio and Radar Telescope Systems*, MIT Press, Cambridge, Massachusetts, USA, 2003.

[98] S. Feng, C. Wang, B. Duan, and Y Ban, "Design of tipping structure for 110 m high-precision radio telescope," *Acta Astronautica*, vol. 141, no. dec, pp. 50–56, 2017.

[99] P. T. P. Ho, P. Altamirano, C. H. Chang et al., "The Yuan-Tseh Lee array for microwave background anisotropy," *The Astrophysical Journal*, vol. 694, no. 2, pp. 1610–1618, 2009.

[100] S. Feng, X. Duan, and B. Duan, "A novel design of large full-steerable reflector antenna," *Sci Sin-Phys Mech Astron*, vol. 47, no. 5, (in Chinese), Article ID 059509, 2017.

[101] S. Feng, Y. Ban, B. Duan, C. Wang, and B Wang, "Electronic performance-oriented mold sharing method and application in QTT 110 m large radio telescope," *IEEE Transactions on Antennas and Propagation*, vol. 68, no. 8, pp. 6407–6412, 2020.

[102] J. Ruze, "Antenna tolerance theory—A review," *Proceedings of the IEEE*, vol. 54, no. 4, pp. 633–640, 1966.

[103] N. Li, J. Wu, B. Y. Duan, and C. S Wang, "Effect of the rail unevenness on the pointing accuracy of large radio telescope," *Acta Astronautica*, vol. 132, pp. 13–18, 2017.

[104] Y. Ban, C. Wang, S. Feng, B. Duan, and W Wang, "Iteration path-length error correction approach to subreflector shaping for distortion compensation of large reflector antenna," *IEEE Transactions on Antennas and Propagation*, vol. 67, no. 4, pp. 2729–2734, 2019.

[105] A. Greve and B. G. Hooghoudt, "Quality evaluation of radio reflector surfaces," *Astronomy and Astrophysics*, vol. 93, pp. 76–78, 1981.

[106] P. Lian, M. Zhu, W. Wang et al., "Estimation method of temperature field of large axial symmetric reflector antenna in real-time," *Journal of Mechanical Engineering*, vol. 51, no. 6, pp. 165–172, 2015, in Chinese.

[107] A. Greve, M. Bremer, J. Penalver, P. Raffin, and D Morris, "Improvement of the IRAM 30-m telescope from temperature measurements and finite-element calculations," *IEEE Transactions on Antennas and Propagation*, vol. 53, no. 2, pp. 851–860, 2005.

[108] A. Greve and D. Morris, "Repetitive radio reflector surface deformations," *IEEE Transactions on Antennas and Propagation*, vol. 53, no. 6, pp. 2123–2126, 2005.

[109] C. S. Wang, Y. F. Yan, Q. Xu et al., "Edge sensor based real-time calculation method for active panel position of QTT," *Research in Astronomy and Astrophysics*, vol. 20, no. 11, p. 182, 2020.

[110] C. S. Wang, B. Y. Duan, and Y. Y. Qiu, "Accurate algorithm for analysis of surface errors in reflector antennas and calculation of gain loss,"vol. 2, pp. 1365–1368, in *Proceedings of the 2005 IEEE International Symposium on Microwave, Antenna, Propagation and EMC Technologies for Wireless Communications*, vol. 2, pp. 1365–1368, IEEE, Beijing, China, August 2005.

[111] A. Orfei, G. Maccaferri, S. Mariotti et al., "The upgrade proposal for the VLBI Medicina antenna," *VLBI TecnologyY: Progress and Future Observational Possibilities*, vol. 165, 170 pages, 1994.

[112] A. Orfei, M. Morsiani, G. Zacchiroll, G. Maccaferri, J. Roda, and F Fiocchi, "An active surface for large reflector antennas," *IEEE Antennas and Propagation Magazine*, vol. 46, no. 4, pp. 11–19, 2004.

[113] Y. Zhang, G. Li, G. Zhou et al., "Real-time closed-loop active surface technology of a large radio telescope," *Publications of the Astronomical Society of the Pacific*, vol. 134, no. 1031, Article ID 015003, 2022.

[114] B. Xiang, N. Wang, M. Chen et al., "Subreflector adjustment system for NSRT," *Ground-based and Airborne Telescopes VII*, International Society for Optics and Photonics, vol. 10700, Article ID 107002E, 2018.

[115] G. Kazezkhan, B. Xiang, N. Wang, and A Yusup, "Dynamic modeling of the Stewart platform for the NanShan radio telescope," *Advances in Mechanical Engineering*, vol. 12, no. 7, Article ID 168781402094007, 2020.

[116] S. Von Hoerner and W. Y. Wong, "Improved efficiency with a mechanically deformable subreflector," *IEEE Transactions on Antennas and Propagation*, vol. 27, no. 5, pp. 720–723, 1979.

[117] J. Antebi, M. S. Zarghamee, F. W. Kan, H. Hartwell, J. Salah, and S Milner, "A deformable subreflector for the Haystack radio telescope," *IEEE Antennas and Propagation Magazine*, vol. 36, no. 3, pp. 19–28, 1994.

[118] U. Bach, "Out of focus holography at effelsberg," in *Proceedings of the 12th European VLBI Network Symposium and Users Meeting (EVN 2014)*, Cagliari, Italy, October 2014.

[119] S. Xu, Y. Rahmat-Samii, and W. A. Imbriale, "Subreflectarrays for reflector surface distortion compensation," *IEEE Transactions on Antennas and Propagation*, vol. 57, no. 2, pp. 364–372, 2009.

[120] P. Lian, W. Wang, and N. Hu, "Feed adjustment method of reflector antenna based on far field," *IET Microwaves, Antennas & Propagation*, vol. 8, no. 10, pp. 701–707, 2014.

[121] W. A. van Cappellen and L. Bakker, "APERTIF: phased array feeds for the westerbork synthesis radio telescope," in *Proceedings of the 2010 IEEE International Symposium on Phased Array Systems and Technology*, pp. 640–647, Waltham, MA, USA, October 2010.

[122] M. V. Ivashina, O. Iupikov, R. Maaskant, W. A. van Cappellen, and T Oosterloo, "An optimal beamforming strategy for wide-field surveys with phased-array-fed reflector antennas," *IEEE Transactions on Antennas and Propagation*, vol. 59, no. 6, pp. 1864–1875, 2011.

[123] H. Li and R. Nan, "Progress and outlook of FAST," *Chinese Journal of Nature*, vol. 37, no. 6, pp. 424–434, 2015, in Chinese.

[124] S. Xu, Y. Rahmat-Samii, and D. Gies, "Shaped-reflector antenna designs using particle swarm optimization: an example of a direct-broadcast satellite antenna," *Microwave and Optical Technology Letters*, vol. 48, no. 7, pp. 1341–1347, 2006.

[125] S. Karimkashi, A. R. Mallahzadeh, and J. Rashed-Mohassel, "A new shaped reflector antenna for wide beam radiation patterns," in *Proceedings of the 2007 International Symposium on Microwave, Antenna, Propagation and EMC Technologies for Wireless Communications*, pp. 535–538, IEEE, Hangzhou, China, August 2007.

[126] R. C. Gupta, S. K. Sagi, K. P. Raja, N. K. Sharma, and R Jyoti, "Shaped prime-focus reflector antenna for satellite communication," *IEEE Antennas and Wireless Propagation Letters*, vol. 16, pp. 1945–1948, 2017.

[127] C. Wang, H. Li, K. Ying et al., "Active surface compensation for large radio telescope antennas," *International Journal of Antennas and Propagation*, vol. 2018, no. 1, Article ID 3903412, 17 pages, 2018.

[128] W. Wang, C. Wang, B. Duan, G. Leng, and X Li, "Compensation for gravity deformation via subreflector motion of 65 m shaped Cassegrain antenna," *IET Microwaves, Antennas & Propagation*, vol. 8, no. 3, pp. 158–164, 2014.

[129] P. Lian, C. Wang, Q. Xu et al., "Real-time temperature estimation method for electromagnetic performance improvement of a large axisymmetric radio telescope under solar radiation," *IET Microwaves, Antennas & Propagation*, vol. 14, no. 13, pp. 1635–1642, 2020.

[130] C. Wang, Na Wang, P. Lian et al., *Thermal Deformation Compensation Technology for Large Reflector Antennas in High Frequency Bands*, Science Press, Beijing, China, 2018, in Chinese.

[131] L. Fu, L. Yu, J. Tang et al., "Thermal analysis of the backup structure of the Tianma telescope," *Research in Astronomy and Astrophysics*, vol. 22, 2022.

[132] S Garcia and Mario, *Robust Control Engineering:Practical QFT Solutions*, CRC Press, FA, USA, 2017, in Chinese.

[133] W. K. Gawronski, *Modeling and Control of Antennas and Telescopes*, Springer, Berlin, Germany, 2008.

[134] J. Zhang, J. Huang, L. Qiu, and R Song, "Analysis of reflector vibration-induced pointing errors for large antennas subject to wind disturbance: evaluating the pointing error caused by reflector deformation," *IEEE Antennas and Propagation Magazine*, vol. 57, no. 6, pp. 46–61, 2015.

[135] T. Ranka, M. Garcia-Sanz, A. Symmes, J. M. Ford, and T Weadon, "Dynamic analysis of the Green Bank Telescope structure and servo system," *Journal of Astronomical Telescopes, Instruments, and Systems*, vol. 2, no. 1, p. 014001, 2016.

[136] W. Gawronski and K. Souccar, "Control systems of the large millimeter telescope," *IEEE Antennas and Propagation Magazine*, vol. 47, no. 4, pp. 41–49, 2005.

[137] J. Kim, S. Park, and T. S. Jin, "Simplified fuzzy-PID controller of data link antenna system for moving vehicles," in *Proceedings of the Pacific Rim International Conference on Artificial Intelligence*, pp. 1083–1088, Springer, Guilin, China, August 2006.

[138] W. Gawronski, "Design and performance of the Hꝏ controller for the beam-waveguide antennas," Jet Propulsion Laboratory, Benglaru, India, Tech. Rep, 2011.

[139] C. S. Wang, X. Q. Wang, Q. Xu et al., "Preliminary study of regulation technology of wind field distribution on QTT site based on test of equivalent wind field," *Sci Sin-Phys Mech Astron*, vol. 49, no. 9, Article ID 099515, 2019, in Chinese.

[140] P. Towers and B. L. Jones, "Real-time wind field reconstruction from LiDAR measurements using a dynamic wind model and state estimation," *Wind Energy*, vol. 19, no. 1, pp. 133–150, 2016.